Multiaxial Reorientations of ND_4^+ Ions Studied by ^{2}H-NMR Spectroscopy

Z. T. Lalowicz and S. F. Sagnowski

Institute of Nuclear Physics, Radzikowskiego 152, PL 31-342 Kraków, Poland

Z. Naturforsch. **46 a**, 829–840 (1991); received July 11, 1991

The density matrix formalism is used to simulate motional averaging in the ^{2}H-NMR spectra of reorienting ND_4^+ ions. The development of the spectra under increasing jump frequency about a single C_3 or C_2 axis is followed. Next we assume a hierarchy of axes in terms of activation energies sufficient to reach extreme narrowing conditions for some axes before activating jumps about a next one. Primary reorientations about the fastest C_3 or C_2 symmetry axes define the shape of spectra, the width of which is then stepwise reduced by fast reorientations about the subsequent axes in a postulated sequence of statistically uncorrelated jumps.

Key words: Deuteron NMR spectroscopy, Molecular dynamics, Ammonium salts, Ammonium ion reorientations. – PACS number 76.60.

Introduction

Studies of molecular mobility are among classical applications of NMR spectroscopy. The features observed in the spectra result from the strength and the transformation properties of spin interactions. The dipole-dipole interaction defines the spectra of $I=1/2$ spin systems. Very early papers successfully explained the spectra observed for rigid and reorienting H_2O [1], CH_3 [2] and NH_4^+ in a single crystal [3]. Immobile molecule, single axis reorientations or isotropic ones were recognized from the shape and width of the spectra. Temperature of the transition between the motional modes gave a rough estimation of the hindering potential. The transitions, however, occured over a narrow range of temperature, which prevented experimental observations of any intermediate case and made related complex theoretical analysis unattractive.

These limitations result from the small coupling constant and multispin character of dipole-dipole interactions. By switching over to deuterons we acquire a much stronger quadrupole interaction with suitable one-particle transformation properties. Therefore we can observe an evolution of deuteron spectra over a much wider transition range, and thus reorientation rates and details of motional dynamics may be obtained.

Reprint requests to Dr. Z. T. Lalowicz, Institute of Nuclear Physics, Radzikowskiego 152, PL 31-342 Kraków/Poland.

^{2}H-NMR spectroscopy has been developed over the last decade into a method frequently used for studies of dynamical processes in a variety of solid state systems, e.g. of polymers [4] and crystalline amino-acids [5], but also of liquid crystals and lipids [6]. Techniques used are 1D, quadrupole echo, spin alignment echo, and 2D exchange spectroscopies. These techniques provide means for detecting molecular jump rates spanned over 10 decades and for deducing the geometry of slow reorientations. The sensitivities of 1D and QE spectroscopies are restricted to relatively fast motions with correlation times shorter than about 10^{-3} s. The deuteron spin alignment and 2D exchange spectroscopy methods extend the range of observation down to very slow motions [7].

Motional narrowing effects are detectable in the NMR spectra if, on increasing the temperature, the jump frequency becomes comparable with the width of the spectrum. Details of the line shape depend upon the interactions and internal motions related to symmetries of the system and lattice potential.

Jump frequencies may be deduced by comparing simulated spectra with experimental ones. It has always been assumed that the motion can be characterized by a single correlation frequency which follows the Arrhenius law. Situations where two motions about a given axis may simultaneously contribute to the line narrowing were also considered, and the usual approach was to treat them sequentially [8]. In many cases, however, more complex threedimensional motions are composed of uncorrelated rotations or oscillations about noncoincident axes. Series of successive

0932-0784 / 91 / 1000-0829 $ 01.30/0. – Please order a reprint rather than making your own copy.

Dieses Werk wurde im Jahr 2013 vom Verlag Zeitschrift für Naturforschung in Zusammenarbeit mit der Max-Planck-Gesellschaft zur Förderung der Wissenschaften e.V. digitalisiert und unter folgender Lizenz veröffentlicht: Creative Commons Namensnennung-Keine Bearbeitung 3.0 Deutschland Lizenz.

This work has been digitalized and published in 2013 by Verlag Zeitschrift für Naturforschung in cooperation with the Max Planck Society for the Advancement of Science under a Creative Commons Attribution-NoDerivs 3.0 Germany License.

Zum 01.01.2015 ist eine Anpassung der Lizenzbedingungen (Entfall der Creative Commons Lizenzbedingung „Keine Bearbeitung") beabsichtigt, um eine Nachnutzung auch im Rahmen zukünftiger wissenschaftlicher Nutzungsformen zu ermöglichen.

On 01.01.2015 it is planned to change the License Conditions (the removal of the Creative Commons License condition "no derivative works"). This is to allow reuse in the area of future scientific usage.

motions were considered in simulations of ^{2}H-NMR spectra [9].

An analysis of the ^{2}H-NMR spectra of an exchanging pair of deuterons was given by Berglund and Tegenfeld [10]. Single crystal spectra of $Li_2SO_4 \cdot D_2O$, measured in the range $-83\,^\circ$C to $103\,^\circ$C, were fitted with theoretical spectra characterized by correlation times ranging from 10^{-3} down to 10^{-6} s. A similar approach was developed and applied to the reorientation of ND_3 in the D-glycine single crystal [11]. When compared with results on protonated systems, a close correspondence of activation energies was observed, but the preexponential factor was to be reduced by about ten. The two-site exchange was also analysed in detail [12], but experimental results show the correlation frequencies of H_2O and D_2O to be equal at any temperature.

Spectroscopic studies of the CD_3 reorientation attracted attention, and the spectra were calculated for a wide range of correlation frequencies [13]. The usual procedure, however, was to interpret the spectra under extreme narrowing conditions, which has been done for the C_3 jumps [14, 15] or for the 180° flips compared with rotational diffusion [16, 17], as well as for a multisite exchange about a common axis [18]. Reorientations in three dimensions, i.e. about noncoinciding axes, were considered only for molecules with internal degrees of freedom, e.g. trimethylamine [19] or lipids [20]. In these cases internal reorientations and whole molecule motions are independent of each other.

Motional effects in ND_4^+ are delt with in a preliminary contribution of Chiba [21, 22]. Narrow lines were attributed to a full narrowing due to isotropic reorientation and broader spectra were used to fit a theory for one immobile spin $I = 1$ with the quadrupole coupling constant and the asymmetry parameter being the adjustable quantities. But in the latter case an equally high mobility of the ion might be expected. However, as related experimental spectra were observed at elevated temperatures and the isotropic average was anticipated, an explanation involving a deformation of the ammonium ion was postulated. There is no point in arguing about all conclusions presented, although there is one which is still frequently drawn and requires some comment. When a doublet with about 2 kHz splitting was observed for some single crystals of ammonium-d_4 salts, [23] and references therein, deformation was assumed to be the only explanation, though this was not proven.

However, if ion deformation is so common, it should also be detectable at low temperatures. The ^{2}H-NMR single crystal spectra measured at 4.2 K for $(ND_4)_2SnCl_6$ indicate no deviation of ND_4^+ from the perfect tetrahedron shape [24]. Moreover the identical quadrupole interactions for all four deuterons indicate also absence of an external EFG, which may however play a role in the spectra of some low crystalline field symmetry compounds. Many cases of high barrier ammonium compounds measured up to the room temperature supply a variety of spectra with characteristic shapes changing at phase transitions also [25].

We expect a relation between these features in the spectra and a multiaxial reorientation of ND_4^+ in different lattice potentials. In this paper we are going to show a variety of deuteron line shapes for the ammonium ion simulated on the basis of a simple motional model involving reorientations of the undeformable ND_4^+ ion around its symmetry axes.

In Chapter II a theoretical basis for spin dynamics calculations is presented. We use the statistical Liouville-von Neumann [26] equation, where quantum evolution of the spin system is governed by a proper spin Hamiltonian, and motional processes are described by respective jump rates.

A motional model for ammonium ion in a crystal lattice is given in Chapter III. It assumes jump reorientations of the ammonium tetrahedron around its symmetry axes. Other kinds of movements, such as two-spin exchange or diffusive rotations, are excluded. ^{2}H-NMR spectra of ND_4^+ calculated for lattice potentials of specific symmetries are given. First an evolution of spectra on increasing frequency of jumps about a C_3 or C_2 symmetry axis is shown. Then as a hierarchy of axes in terms of activation energy is assumed, the applied procedure of simulations involve a stepwise transition to extreme narrowing conditions for consecutive rotation axes. Characteristic shapes of spectra are discussed, each being attributed to a sequence of jumps about several symmetry axes of the ion. Chapter IV recalls some previously published experimental spectra of ND_4^+ ions at high temperatures and gives a new interpretation of the spectra based on our motional model. The dynamical state of ND_4^+ ion is discussed for each spectrum.

II. Spin Dynamics Calculations

Consider an ensemble of spin systems, each composed of n identical spins I performing jumps between

N orientations. Jumps are assumed to be sudden and as such leave the state of the system unchanged with only its Hamiltonian altered. Between two consecutive jumps the spin system remains fixed in space, so its time development is governed by a time independent Hamiltonian appropriate to actual orientation.

At any time t we may consider the whole ensemble to be composed of N subensembles each containing spin systems in one of the N orientations. The normalized density matrix $\varrho(t)$ of the full ensemble is

$$\varrho(t) = \sum_{\mu=1}^{N} p_\mu \varrho^\mu(t), \tag{1}$$

where ϱ^μ is the normalized density matrix of the subensemble of spin systems which at time t have the orientation μ, while p_μ is the fraction of spin systems having this orientation and $\sum_\mu p_\mu = 1$. We assume p_μ to be constant in time as a result of dynamical equilibrium which requires

$$p_\mu W_{\mu\nu} = p_\nu W_{\nu\mu},$$

where $W_{\mu\nu}$ is the probability of the spin system for jumping from the orientation μ to ν.

We are going to calculate the NMR signal

$$S(t) = \mathrm{Tr}(\varrho I_x) = \sum_{\mu=1}^{N} \mathrm{Tr}(p_\mu \varrho^\mu I_x) = \sum_{\mu i j} p_\mu \varrho_{ij}^\mu (I_x^*)_{ij} \tag{2}$$

with $i, j = 1, \ldots (2I+1)^n$.

The order of summed up terms of course is irrelevant, but some ordering may be convenient. Once a particular order has been chosen, we may write

$$S(t) = \sum_s \mathcal{T}_s \varrho_s = \vec{\mathcal{T}} \cdot \vec{\varrho}, \tag{3}$$

where $\varrho_s = \varrho_{ij}^\mu$ and $\mathcal{T}_s = (I_x^*)_{ij} p_\mu$.

Each matrix element I_{xij}^* appears N times in $\vec{\mathcal{T}}$ although with different coefficients p_μ.

The time dependence of the partial density matrix ϱ^μ is given by N differential matrix equations

$$\dot{\varrho}^\mu = -i[\mathcal{H}^\mu, \varrho^\mu] + \sum_{\nu \neq \mu} W_{\nu\mu} \varrho^\nu - \left(\sum_{\nu \neq \mu} W_{\mu\nu}\right) \varrho^\mu, \tag{4}$$

$$\mu, \nu = 1, \ldots, N,$$

where $\mathcal{H}^\mu$ is the Hamiltonian of the spin system at the orientation μ.

The commutator in (4) involves spin interactions and is sometimes called the quantum motion term. The two remaining terms describe the classical motion of the spin systems, and the probabilities $W_{\mu\nu}$ have to be derived from the assumed motional model.

Equations (4), except for special cases when analytical solution is possible [12], have to be solved numerically. In the following we propose a convenient formalism.

As the dimension of the spin representation is $(2I+1)^n$ and $\mu = 1, \ldots, N$ spatial positions, the set of $(2I+1)^{2n} N$ equations in (4) may be written in vector form:

$$\dot{\vec{\varrho}} = \mathcal{A} \vec{\varrho}. \tag{5}$$

Note that for four interacting deuterons in ND_4^+ we have $n = 4$, $N = 12$, $I = 1$ and $(2I+1)^{2n} N = 78732$. In the next Chapter, however, we shall show that the problem may be reduced to the dimension 4.

We may find a time independent matrix T which diagonalizes $\mathcal{A}$, i.e. $\mathcal{A}' = T \mathcal{A} T^{-1}$, $\vec{\varrho}' = T\vec{\varrho}$, thus receiving a set of uncoupled equations

$$\dot{\vec{\varrho}}' = \mathcal{A}' \vec{\varrho}'. \tag{6}$$

Solutions are found now in the form

$$\varrho'(t) = \varrho_s'(0) \exp(\mathcal{A}_s' t), \tag{7}$$

Since the matrix $\mathcal{A}$ is not Hermitian, its eigenvalues $\mathcal{A}_s$ do not have to be real, and in general $\mathcal{A}_s' = -a_s + i\omega_s$. Introducing $\vec{\mathcal{T}}' = (T^{-1})^\dagger \vec{\mathcal{T}}$ we may rewrite (3) as

$$S(t) = \vec{\mathcal{T}}' \cdot \vec{\varrho}' = M_0 \sum_s C_s \exp(i\phi_s) \exp(-a_s + i\omega_s) t, \tag{8}$$

where $C_s \exp(i\phi_s) = \mathcal{T}_s' \varrho_s'(0)$.

The NMR spectrum $I(\omega)$ is obtained by a Fourier transform of $S(t)$:

$$I(\omega) = \tfrac{1}{2} \sum_s C_s \{\cos\phi_s [L(\omega - \omega_s) + L(\omega + \omega_s)] + \sin\phi_s [Q(\omega - \omega_s) - Q(\omega + \omega_s)]\}, \tag{9}$$

where $L(x) = \frac{1}{\pi} a_s (a_s^2 + x^2)^{-1}$ and $Q(x) = \frac{1}{\pi} x (a_s^2 + x^2)^{-1}$.

As $\mathcal{H}^\mu$ depends on the orientation with respect to the external magnetic field $\vec{B}_0$, the calculations leading to a powder spectrum have to be repeated for a grid of (Θ, ϕ) angles over the ranges required by the symmetry.

III. Theory of ND_4^+ Spectra

III.1. Motional Model

As an ensemble of spin systems we consider now ND_4^+ ions in a crystal lattice. We assume that the ammonium ion is an undeformable perfect tetrahe-

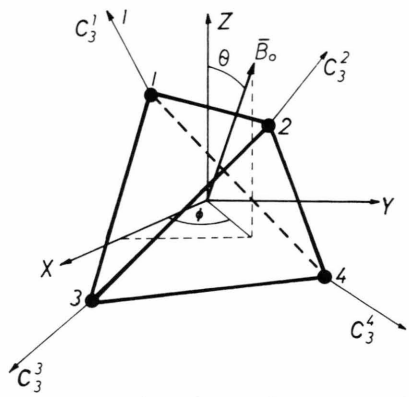

Fig. 1. Molecular reference frame x, y, z for ND_4^+ ion.

dron. The ammonium ion interacts with neighbouring ions. Interactions involve hydrogens and tend to locate them around minimum potential positions. Thermally activated jumps are possible between neighbouring equilibrium positions. We consider jumps about the symmetry axes of the ion only, against eventually different barrier heights. They are 120° rotations around threefold axes and 180° rotations around twofold axes. Any diffusive rotations characterized by a continuous change of a rotation angle are excluded. In Fig. 1 a molecular reference frame $x\,y\,z$ is shown along with ND_4^+ deuterons labeled 1, 2, 3, 4. Four C_3 axes pass through the four corners of the tetrahedron and three C_2 axes coincide with the x, y and z axes of the frame. Symmetry jumps are thermally activated, i.e. the jump frequency Ω depends on temperature T and lattice potential barrier E_a according to the Arrhenius law

$$\Omega = \Omega_0 \exp(-E_a/RT). \tag{10}$$

We introduce Ω_k ($k = 1, 2, 3, 4, x, y, z$) for jump frequencies about the C_3 and C_2 symmetry axes, respectively.

III.2. Deuteron Spin Interactions

The dominating spin interaction is the coupling of the deuteron quadrupole moment Q to the electric field gradient (EFG) $\vec{V}$ at a deuteron. The EFG experienced by the deuterons in the four sites of ND_4^+ is axially symmetric with its local symmetry axis along an N–D bond and principal value $V_{zz} = e\,q$. The quadrupole coupling constant $C_Q = e^2\,q\,Q\,h^{-1}$ amounts to 180 kHz, consistently measured for a number of ammonium salts.

Deuteron dipole-dipole interactions, being much weaker than the quadrupole ones, will be neglected in this consideration. This makes all four deuterons in ND_4^+ equivalent and allows us to trace movements of the ion by observing one deuteron in each ion only. The size of the problem is thus significantly reduced, as we now have the number of spins in the spin system $n = 1$ and four possible deuteron positions ($N = 4$).

The external magnetic field $\vec{B}_0$ is assumed strong enough to consider the secular part of the quadrupole Hamiltonian only. Thus for the i-th deuteron site in ND_4^+ we have

$$\mathcal{H}_Q^i = \tfrac{1}{8} C_Q (3\cos^2\theta_i - 1)[3I_z^2 - I(I+1)] = \nu_Q F_i^0 T_{20}, \tag{11}$$

where θ_i is the angle between $\vec{B}_0$ and the N–D^i direction.

The orientation of $\vec{B}_0$ is given by polar angles θ, ϕ (see Fig. 1), and for respective deuteron sites we have the following expressions:

$$\begin{aligned}
F_1^0 &= \sin\theta[\sin\theta\sin 2\phi + 2\cos\theta(\sin\phi + \cos\phi)],\\
F_2^0 &= \sin\theta[\sin\theta\sin 2\phi - 2\cos\theta(\sin\phi + \cos\phi)],\\
F_3^0 &= \sin\theta[-\sin\theta\sin 2\phi - 2\cos\theta(\sin\phi - \cos\phi)],\\
F_4^0 &= \sin\theta[-\sin\theta\sin 2\phi + 2\cos\theta(\sin\phi - \cos\phi)].
\end{aligned} \tag{12}$$

III.3. Calculation of Spectra

Each of the deuterons in the ammonium ion contributes a pair of lines in the spectrum. The doublet separation $\Delta\nu$ takes values in the range $-\frac{3}{8}\nu_Q \leqq \Delta\nu \leqq \frac{3}{4}\nu_Q$, depending on the orientation with respect to the direction of $\vec{B}_0$. In this range the spectral components are found in powder spectra. A doublet with the separation $\Delta\nu_{rig} = \frac{3}{4}\nu_Q$ strongly dominates the powder spectrum.

As there is no preference of any orientation of ND_4^+, p_μ in (1) are all equal. Thus (1) assumes the form

$$\varrho(t) = \frac{1}{4}\sum_{\mu=1}^{4}\varrho^\mu(t). \tag{13}$$

Similarly, (4) transforms into a set of four matrix equations

$$\dot{\varrho}^\mu = -i[\mathcal{H}_Q^\mu, \varrho^\mu] + \sum_{\nu\neq\mu} W_{\nu\mu}\varrho^\nu - \Big(\sum_{\nu\neq\mu} W_{\mu\nu}\Big)\varrho^\mu, \qquad \mu, \nu = 1, \ldots, 4, \tag{14}$$

where $W_{\mu\nu}$ is now the probability of deuteron jumps from site μ to ν according to the ammonium ion symmetry rotations. Thus they are related to jump rates

Ω_k as follows:

$$W_{12}=\Omega_3+\Omega_4+\Omega_z, \quad W_{13}=\Omega_2+\Omega_4+\Omega_y,$$
$$W_{14}=\Omega_2+\Omega_3+\Omega_x, \quad W_{23}=\Omega_1+\Omega_4+\Omega_x, \tag{15}$$
$$W_{24}=\Omega_1+\Omega_3+\Omega_y, \quad W_{34}=\Omega_1+\Omega_2+\Omega_z.$$

The NMR signal $S(t)$ is expressed by

$$S(t)=\frac{1}{4}\sum_{\mu=1}^{4}\mathrm{Tr}(\varrho^{\mu}I_x). \tag{16}$$

For one spin $I=1$, ϱ^{μ} and I_x are given by 3×3 matrices, and in I_z eigenfunction base we have

$$I_x=\frac{1}{\sqrt{2}}\begin{pmatrix}0&1&0\\1&0&1\\0&1&0\end{pmatrix}, \tag{17}$$

and then (16) becomes

$$S(t)=\frac{\sqrt{2}}{4}\sum_{\nu=1}^{4}\mathrm{Re}(\varrho_{12}^{\mu}+\varrho_{23}^{\mu}). \tag{18}$$

Similarly, the spin operator appearing in (11) is given by

$$T_{20}=\begin{pmatrix}1&0&0\\0&-2&0\\0&0&1\end{pmatrix} \tag{19}$$

and thus the element (i, k) of the commutator in (14) is simply

$$[\mathscr{H}_{\mathrm{Q}}^{\mu}, \varrho^{\mu}]_{ik}=\nu_{ik}^{\mu}\varrho_{ik}^{\mu} \tag{20}$$

with $\nu_{12}^{\mu}=-3\nu_{\mathrm{Q}}F_{\mu}^{0}$, $\nu_{23}^{\mu}=-\nu_{12}^{\mu}$, and $\nu_{13}^{\mu}=0$. Note that due to the diagonal form of T_{20} there is no coupling between matrix elements ϱ_{ik}^{μ} of different indices, and (14) transforms into nine independent sets of four coupled differential equations:

$$\dot{\varrho}_{ik}^{\mu}=-i\nu_{ik}^{\mu}\varrho_{ik}^{\mu}+\sum_{\nu\neq\mu}W_{\nu\mu}\varrho_{ik}^{\nu}-\Big(\sum_{\nu\neq\mu}W_{\mu\nu}\Big)\varrho_{ik}^{\mu}; \tag{21}$$
$$i, k=1, \ldots, 3;\ \mu, \nu=1, \ldots, 4.$$

Moreover $\nu_{23}^{\mu}=-\nu_{12}^{\mu}$ implies $\varrho_{23}^{\mu}=\varrho_{12}^{\mu *}$, and this simplifies (20) into

$$S(t)=\frac{1}{\sqrt{2}}\sum_{\mu=1}^{4}\mathrm{Re}\,\varrho_{12}^{\mu}. \tag{22}$$

Finally, we must find only four matrix elements ϱ_{12}^{μ} and only one set of equations (21) has to be solved. Putting $\varrho_{\mu}=\varrho_{12}^{\mu}$ and $\nu_{\mu}=\nu_{12}^{\mu}$ and making use of (15), we rewrite (21) in the form

$$\begin{aligned}\dot{\varrho}_1=&-i\nu_1\varrho_1+\Omega_2(\varrho_3+\varrho_4-2\varrho_1)+\Omega_3(\varrho_2+\varrho_4-2\varrho_1)\\&+\Omega_4(\varrho_2+\varrho_3-2\varrho_1)+\Omega_x(\varrho_3-\varrho_1)\\&+\Omega_y(\varrho_4-\varrho_1)+\Omega_z(\varrho_2-\varrho_1),\end{aligned}$$

$$\begin{aligned}\dot{\varrho}_2=&-i\nu_2\varrho_2+\Omega_1(\varrho_3+\varrho_4-2\varrho_2)+\Omega_3(\varrho_1+\varrho_4-2\varrho_2)\\&+\Omega_4(\varrho_1+\varrho_3-2\varrho_2)+\Omega_x(\varrho_4-\varrho_2)\\&+\Omega_y(\varrho_3-\varrho_2)+\Omega_z(\varrho_1-\varrho_2),\end{aligned} \tag{23}$$

$$\begin{aligned}\dot{\varrho}_3=&-i\nu_3\varrho_3+\Omega_1(\varrho_2+\varrho_4-2\varrho_3)+\Omega_2(\varrho_1+\varrho_4-2\varrho_3)\\&+\Omega_4(\varrho_1+\varrho_2-2\varrho_3)+\Omega_x(\varrho_1-\varrho_3)\\&+\Omega_y(\varrho_2-\varrho_3)+\Omega_z(\varrho_4-\varrho_3),\end{aligned}$$

$$\begin{aligned}\dot{\varrho}_4=&-i\nu_4\varrho_4+\Omega_1(\varrho_2+\varrho_3-2\varrho_4)+\Omega_2(\varrho_1+\varrho_3-2\varrho_4)\\&+\Omega_3(\varrho_1+\varrho_2-2\varrho_4)+\Omega_x(\varrho_2-\varrho_4)\\&+\Omega_y(\varrho_1-\varrho_4)+\Omega_z(\varrho_3-\varrho_4),\end{aligned}$$

which is most convenient for the further discussion.

The NMR line shape depends on the relative magnitudes of the linewidth $\Delta\nu$ and jump rates Ω_k. Molecular reorientation at $\Omega_k\ll\Delta\nu$ has no influence on the spectrum. Therefore in the general equations (23) we can neglect all terms with the respective Ω_k. When this is the case for all k, we obtain the rigid lattice spectrum. For any $\Omega_k\sim\Delta\nu$ the spectrum shows effects of motional narrowing. The powder spectrum is rather broad, and therefore for moderate jump frequencies the narrowing condition is fulfilled to a different extent for various doublets. In this sense the ^{2}H-NMR spectrum of ND_4^+ narrows inhomogeneously.

Primary C_3 Axis Jumps

In order to make our approach to multiaxial rotations clear we first assume that the only possible motions appear about the threefold axes, so $\Omega_x=\Omega_y=\Omega_z=0$. Moreover, we assume that heights of all four barriers hindering the C_3 rotations are different, say $E_{a1}<E_{a2}<E_{a3}<E_{a4}$ so that, according to (10), $\Omega_1\gg\Omega_2\gg\Omega_3\gg\Omega_4$ at any temperature well above absolute zero.

Cases in which twofold rotations take place as well as those where activation energies for different rotation axes are equal will be considered later.

At absolute zero all Ω_k are zero and the spectrum calculated with (23) is a rigid lattice one. Its shape, determined only by quantum spin terms $-i\nu_{\mu}\varrho_{\mu}$, is a familiar Pake's doublet of the width $\Delta\nu_{\mathrm{rig}}=135$ kHz. Jump frequencies increase when temperature raises but as far as $\Omega_k\ll\Delta\nu_{\mathrm{rig}}$, classical motion terms in (23) may be neglected and still the rigid lattice spectrum is obtained.

When the temperature increases and Ω_1 becomes comparable with $\Delta\nu_{\mathrm{rig}}$ (while the remaining jump rates

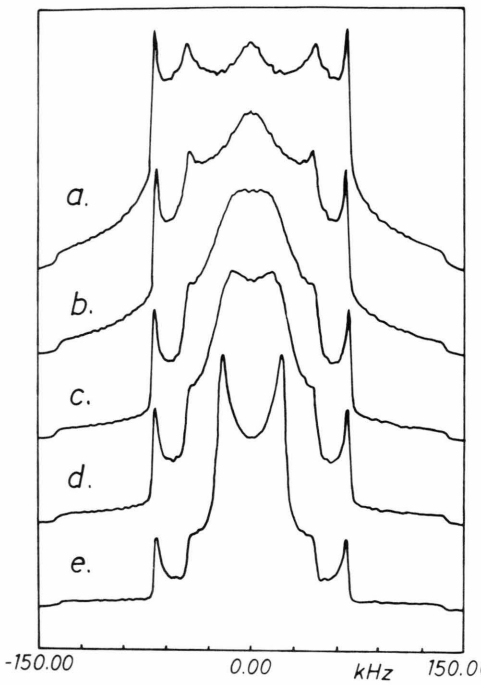

Fig. 2. Theoretical ^{2}H-NMR spectra of ND_4^+ ions performing 120° jumps about $C_3^{(1)}$ symmetry axis calculated for different jump frequencies Ω_1: a) $\Omega_1 = 15$ kHz, b) $\Omega_1 = 30$ kHz, c) $\Omega_1 = 80$ kHz, d) $\Omega_1 = 120$ kHz, e) $\Omega_1 = 600$ kHz.

are still much smaller than $\Delta\nu_{\text{rig}}$) we are dealing with the case of one axis rotation. In Fig. 2 the evolution of the NMR spectrum calculated for increasing Ω_1 is shown. Already at low jump frequencies three peaks emerge at 0, ± 45 kHz. There are two orientations of ND_4^+ at which deuterons jump between positions of exactly equal quadrupole shifts ($\vec{B}_0 \parallel C_2$, $\vec{B}_0 \parallel C_3^{(1)}$), and the motion causes no fluctuation of the interaction. All but these spectral components broaden, which is due to the motional fluctuation of the quadrupole interaction. On increasing the jump rate, a central component builds up and changes its shape from a round top to a doublet with a reduced separation.

For the temperature range where $\Omega_1 \gg \Delta\nu_{\text{rig}}$, and where simultaneously all remaining jump frequencies are still much smaller than $\Delta\nu_{\text{rig}}$, a line shape is reached which does not change with further increase in Ω_1. The spectrum is composed of two doublets: one a rigid lattice doublet with the relative intensity equal to 1/4, and the other, a similar doublet of three times reduced width and an intensity equal to 3/4 (see Figure 2e). We introduce the symbol $1\,C_3^{\infty}$ for this spectrum. The width of the full spectrum is $\Delta\nu = \frac{1}{3}\Delta\nu_{\text{rig}}$.

A further increase of Ω_1 does not influence the spectrum. Below we are going to show that in this case (23) has to be written in an equivalent form in which the parameter Ω_1 is not explicit although the fast motion around the $C_3^{(1)}$ axis has been taken into account.

With the assumption $\Omega_k \ll \Delta\nu_{\text{rig}}$ for $k = 2, 3, 4$, all terms with Ω_2, Ω_3, and Ω_4 can be omitted in (23) and we are left with the following set of equations:

$$\begin{aligned}
\dot{\varrho}_1 &= -i\nu_1\varrho_1, \\
\dot{\varrho}_2 &= -i\nu_2\varrho_2 + \Omega_1(\varrho_3 + \varrho_4 - 2\varrho_2), \\
\dot{\varrho}_3 &= -i\nu_3\varrho_3 + \Omega_1(\varrho_2 + \varrho_4 - 2\varrho_3), \\
\dot{\varrho}_4 &= -i\nu_4\varrho_4 + \Omega_1(\varrho_2 + \varrho_3 - 2\varrho_4).
\end{aligned} \tag{24}$$

The second, third and the fourth equations (24) are coupled by Ω_1 motion, while the first one is not coupled to any of the them and thus supplies the spectrum of the immobile deuteron. As the solution of the first equation is straightforward, let us consider the remaining three. We sum them up receiving

$$\dot{\varrho}_2 + \dot{\varrho}_3 + \dot{\varrho}_4 = -i(\nu_2\varrho_2 + \nu_3\varrho_3 + \nu_4\varrho_4), \tag{25}$$

which is the equation for the quantity $(\varrho_2 + \varrho_3 + \varrho_4)$ not depending on Ω_1. On the other hand $\Omega_1 \gg \Delta\nu_{\text{rig}}$, so we can drop in (24) all spin interaction terms, $-i\nu_\mu\varrho_\mu$, reaching the approximate form

$$\begin{aligned}
\dot{\varrho}_2 &= \Omega_1(\varrho_3 + \varrho_4 - 2\varrho_2), \\
\dot{\varrho}_3 &= \Omega_1(\varrho_2 + \varrho_4 - 2\varrho_3), \\
\dot{\varrho}_4 &= \Omega_1(\varrho_2 + \varrho_3 - 2\varrho_4).
\end{aligned} \tag{26}$$

It requires that $\varrho_2 = \varrho_3 = \varrho_4$, which is easy to show if we find that the equation

$$\dot{\varrho}_k - \dot{\varrho}_j = -3\Omega_1(\varrho_k - \varrho_j) \quad \text{for} \quad k, j = 2, 3, 4 \tag{27}$$

is valid. Its solution is

$$\varrho_k - \varrho_j = [\varrho_k(0) - \varrho_j(0)]\exp(-3\Omega_1 t). \tag{28}$$

But $\varrho_1(0) = \varrho_2(0) = \varrho_3(0) = \varrho_4(0)$, because after the $\pi/2$ pulse all spins of the system are in the same state. Thus for large Ω_1 we have the equality: $\varrho_k = \varrho_j$ for $k, j = 2, 3, 4$. Now we can use this in (25) obtaining

$$\dot{\varrho}_k = -i\bar{\nu}^{(1)}\varrho_k \quad \text{for} \quad k = 2, 3, 4, \tag{29}$$

where $\bar{\nu}^{(1)} = \frac{1}{3}(\nu_2 + \nu_3 + \nu_4) = -\frac{1}{3}\nu_1$. The conclusion is that the fast rotation about one axis results in the equality of the density matrices involved and the averaging of the corresponding frequencies. So the equiva-

lent form of (23) for the fast rotation about $C_3^{(1)}$ axis is

$$\begin{aligned}
\dot{\varrho}_1 &= -i\nu_1\varrho_1 \quad +\Omega_2(\varrho_3+\varrho_4-2\varrho_1)+\Omega_3(\varrho_2+\varrho_4-2\varrho_1)+\Omega_4(\varrho_2+\varrho_3-2\varrho_1),\\
\dot{\varrho}_2 &= -i\bar{\nu}^{(1)}\varrho_2 \qquad\qquad +\Omega_3(\varrho_1+\varrho_4-2\varrho_2)+\Omega_4(\varrho_1+\varrho_3-2\varrho_2),\\
\dot{\varrho}_3 &= -i\bar{\nu}^{(1)}\varrho_3+\Omega_2(\varrho_1+\varrho_4-2\varrho_3) \qquad\qquad +\Omega_4(\varrho_1+\varrho_2-2\varrho_3),\\
\dot{\varrho}_4 &= -i\bar{\nu}^{(1)}\varrho_4+\Omega_2(\varrho_1+\varrho_3-2\varrho_4)+\Omega_3(\varrho_1+\varrho_2-2\varrho_4).
\end{aligned} \tag{30}$$

A further increase of the temperature does not change the spectrum until Ω_2 becomes comparable with $\frac{1}{3}\Delta\nu_{\mathrm{rig}}$. Then, with increasing Ω_2, the line shape changes as shown in Figure 3.

When the temperature reaches the range where $\Omega_2 \gg \frac{1}{3}\Delta\nu_{\mathrm{rig}}$, the spectrum becomes insensitive to any further increase of Ω_2. The line shape is similar to that of the $1C_3^{\infty}$ case but its width is now three times smaller: the separations of two doublets are now $\frac{1}{3}\Delta\nu_{\mathrm{rig}}$ and $\frac{1}{9}\Delta\nu_{\mathrm{rig}}$ with the integral intensity ratio 1:3. The symbol of this spectrum in our notation is $2C_3^{\infty}$. For the mathematical description of this case, (30) has to be written in an equivalent form, which can be obtained in a similar way as those for the rotation about $C_3^{(1)}$ axis. They are

$$\begin{aligned}
\dot{\varrho}_1 &= -i\bar{\nu}^{(2)}\varrho_1+\Omega_3(\varrho_2+\varrho_4-2\varrho_1)+\Omega_4(\varrho_2+\varrho_3-2\varrho_1),\\
\dot{\varrho}_2 &= -i\bar{\nu}^{(1)}\varrho_2+\Omega_3(\varrho_1+\varrho_4-2\varrho_2)+\Omega_4(\varrho_1+\varrho_3-2\varrho_2),\\
\dot{\varrho}_3 &= -i\bar{\nu}^{(2)}\varrho_3 \qquad\qquad +\Omega_4(\varrho_1+\varrho_2-2\varrho_3),\\
\dot{\varrho}_4 &= -i\bar{\nu}^{(2)}\varrho_4+\Omega_3(\varrho_1+\varrho_2-2\varrho_4)
\end{aligned} \tag{31}$$

with $\bar{\nu}^{(2)} = \frac{1}{3}(\nu_1+2\bar{\nu}^{(1)}) = \frac{1}{9}\nu_1$. We have omitted here all terms with Ω_2 in the first, third and the fourth equations of (30). We have, however, taken into account the fast rotation about the $C_3^{(2)}$ axis by putting in the appropriate average frequency $\bar{\nu}^{(2)}$.

The process of activation of the remaining two threefold axes with increasing temperature is straightforward. In the extreme narrowing limit for the additional $C_3^{(3)}$ axis the first, second and the fourth of equations (31) are involved in averaging. They become

$$\begin{aligned}
\dot{\varrho}_1 &= -i\bar{\nu}^{(3)}\varrho_1+\Omega_4(\varrho_2+\varrho_3-2\varrho_1),\\
\dot{\varrho}_2 &= -i\bar{\nu}^{(3)}\varrho_2+\Omega_4(\varrho_1+\varrho_3-2\varrho_2),\\
\dot{\varrho}_3 &= -i\bar{\nu}^{(2)}\varrho_3+\Omega_4(\varrho_1+\varrho_2-2\varrho_3),\\
\dot{\varrho}_4 &= -i\bar{\nu}^{(3)}\varrho_4,
\end{aligned} \tag{32}$$

and the average frequency in this case is $\bar{\nu}^{(3)} = \frac{1}{3}(\bar{\nu}^{(1)}+2\bar{\nu}^{(2)}) = -\frac{1}{27}\nu_1$.

For the extreme narrowing with the last threefold axis, $C_3^{(4)}$, the first three equations of (32) take part in averaging and the final average frequency is $\bar{\nu}^{(4)} =$

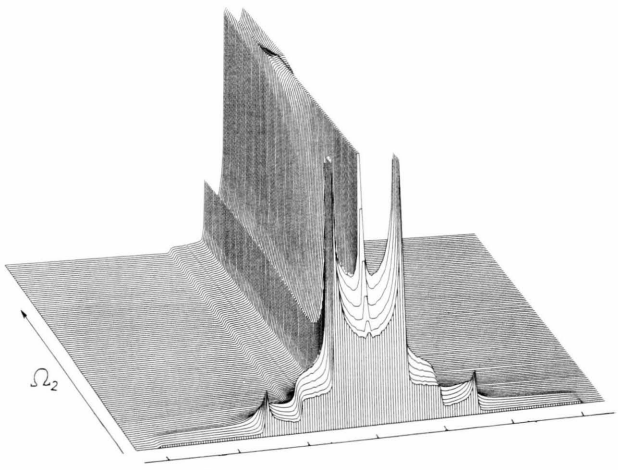

Fig. 3. Evolution of ^{2}H-NMR spectrum on increasing jump frequency Ω_2 about successive $C_3^{(2)}$ axis. Consecutive spectra correspond to Ω_2 increasing according to the formula $\Omega_2(n) = \exp(-1/T_n)$ [MHz], where $T_n = 0.08 + 0.013\,n$. Scale 45 kHz/division.

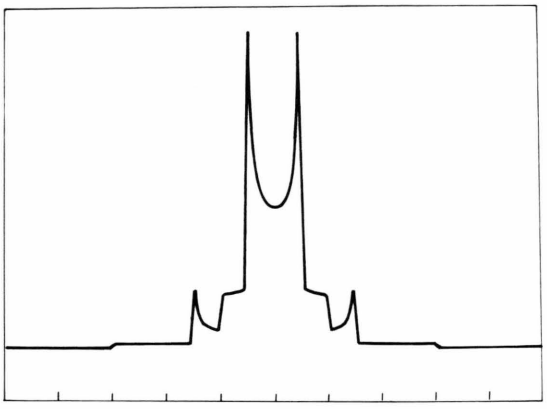

Fig. 4. Standard ^{2}H-NMR spectrum of ND_4^+ ion performing fast multiaxis reorientation. The quadrupole coupling constant 180 kHz was assumed. 1. jumps about a single C_3 axis, "$1C_3^{\infty}$" – scale 45 kHz/division, 2. jumps about two C_3 axes, "$2C_3^{\infty}$" – scale 15 kHz/division, 3. jumps about three C_3 axes, "$3C_3^{\infty}$" – scale 5 kHz/division, 4. jumps about four C_3 axes, "$3C_3^{\infty}$" – scale 1.66 kHz/division. Central doublet splitting equals 1 division.

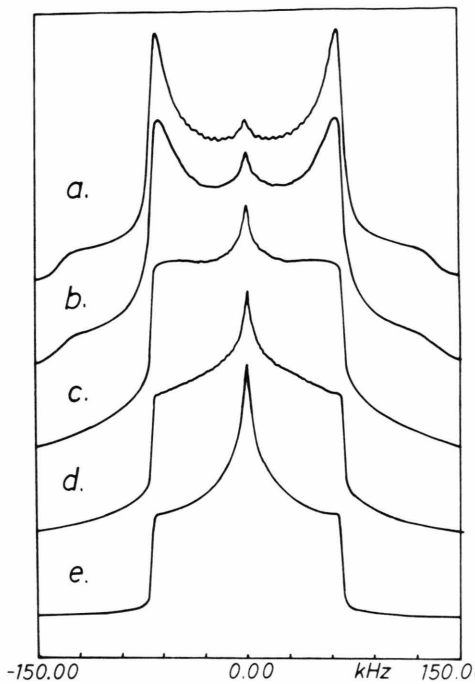

Fig. 5. Theoretical ^{2}H-NMR spectra of ND_4^+ performing 180° jumps about the $C_2^{(x)}$ axis with increasing jump frequency Ω_x: a) $\Omega_x = 5$ kHz, b) $\Omega_x = 10$ kHz, c) $\Omega_x = 30$ kHz, d) $\Omega_x = 70$ kHz, e) $\Omega_x = 300$ kHz.

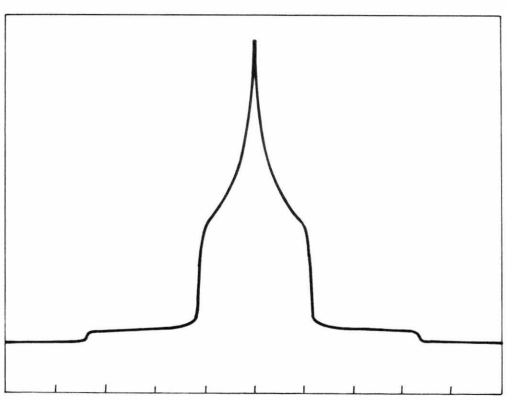

Fig. 6. Pattern spectra of ND_4^+ performing a sequence $1C_2^\infty + nC_3^\infty$ of reorientations is characterized by the width $\delta = 45$ kHz for $n = 1$; $\delta = 15$ kHz for $n = 2$; $\delta = 5$ kHz for $n = 3$; $\delta = 1.66$ kHz for $n = 4$. The broad component disappears for $1C_2^\infty + nC_3^\infty + 1C_2^\infty$.

$\frac{1}{3}(\bar{\nu}^{(2)} + 2\bar{\nu}^{(3)}) = \frac{1}{81}\nu_1$. In both above cases of extreme narrowing the spectrum contains two doublets with the relative intensities 1/4 and 3/4 and the widths $\frac{1}{9}\Delta\nu_{\text{rig}}$ and $\frac{1}{27}\Delta\nu_{\text{rig}}$ (symbol $3C_3^\infty$) for the $C_3^{(3)}$ axis and $\frac{1}{27}\Delta\nu_{\text{rig}}$ and $\frac{1}{81}\Delta\nu_{\text{rig}}$ ($4C_3^\infty$ case, see Figure 4).

In the intermediate ranges i.e. when $\Omega_3 \approx \frac{1}{9}\Delta\nu_{\text{rig}}$ for $C_3^{(3)}$ rotation and when $\Omega_4 \approx \frac{1}{27}\Delta\nu_{\text{rig}}$ for $C_3^{(4)}$ rotation, the line shape changes as shown in Fig. 3 with the appropriate rescaling of the frequency axis.

Activation of any twofold axis after any of the C_3 axes in a chain of consecutive rotations appearing with increasing temperature causes a disappearance of the outer doublet in the spectrum in Fig. 4. For example, if $C_2^{(x)}$ axis jumps become activated after $C_3^{(4)}$ in a sequence of rotations just considered, (23) assumes the final form (we take $\Omega_y = \Omega_z = 0$)

$$\begin{aligned}
\dot{\varrho}_1 &= -i\bar{\nu}^{(4)}\varrho_1 + \Omega_x(\varrho_3 - \varrho_1),\\
\dot{\varrho}_2 &= -i\bar{\nu}^{(4)}\varrho_2 + \Omega_x(\varrho_4 - \varrho_2),\\
\dot{\varrho}_3 &= -i\bar{\nu}^{(4)}\varrho_3 + \Omega_x(\varrho_1 - \varrho_3),\\
\dot{\varrho}_4 &= -i\bar{\nu}^{(3)}\varrho_4 + \Omega_x(\varrho_2 - \varrho_4).
\end{aligned} \tag{33}$$

Rotation around the $C_2^{(x)}$ axis couples equations (33) in pairs: the first with the third and the second with the fourth. In the extreme narrowing limit, i.e. when $\Omega_x \gg \frac{1}{81}\Delta\nu_{\text{rig}}$, all four equations lead to the same line shape (symbol $4C_3^\infty\, 1C_2^\infty$) because the average frequency for the first pair is just $\bar{\nu}^{(4)} = \frac{1}{81}\nu_1$, and for the second pair it is $\frac{1}{2}(\bar{\nu}^{(3)} + \bar{\nu}^{(4)}) = -\frac{1}{81}\nu_1$. The line shape, being symmetric around $\nu = 0$, does not depend on the sign of the frequency term in the Liouville equation (14).

Activation of the consecutive fast rotation about the second twofold axis, say $C_2^{(y)}$, ($4C_3^\infty\, 2C_2^\infty$ case) narrows the spectrum to a single Lorentzian central line. The average frequencies for all four equations in the appropriate differential equations for ϱ_μ are in this case all zero.

Primary C_2 Axis Jumps

An interesting situation appears when the first jumps in a sequence, the most frequent (i.e. against the smallest potential barrier), are performed about one of the twofold axes. Let us assume it is the $C_2^{(x)}$ axis. We start our consideration from the rigid lattice case, i.e. when $\Omega_x \ll \Delta\nu_{\text{rig}}$. With raising temperature we reach the range where $\Omega_x \approx \Delta\nu_{\text{rig}}$, and then the spectrum is described by (23), which for $\Omega_k \ll \Delta\nu_{\text{rig}}$ for $k = 1, 2, 3, 4$, y, z are

$$\begin{aligned}
\dot{\varrho}_1 &= -i\nu_1\varrho_1 + \Omega_x(\varrho_3 - \varrho_1),\\
\dot{\varrho}_2 &= -i\nu_2\varrho_2 + \Omega_x(\varrho_4 - \varrho_2),\\
\dot{\varrho}_3 &= -i\nu_3\varrho_3 + \Omega_x(\varrho_1 - \varrho_3),\\
\dot{\varrho}_4 &= -i\nu_4\varrho_4 + \Omega_x(\varrho_2 - \varrho_4).
\end{aligned} \tag{34}$$

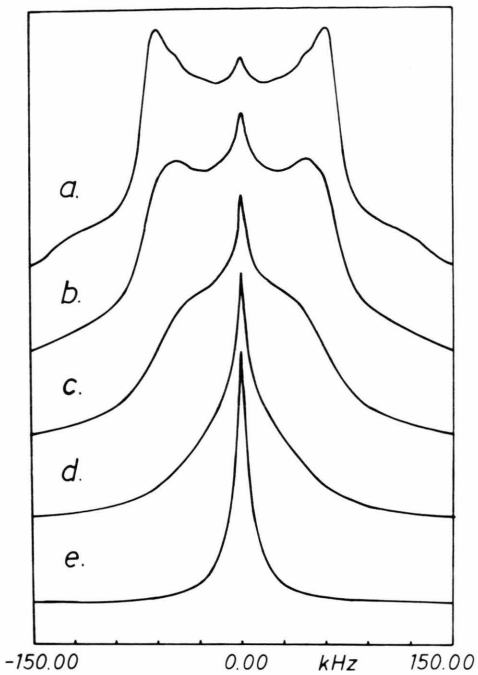

Fig. 7. Theoretical ^{2}H-NMR spectra of ND_4^+ ions performing jumps about two or more equivalent symmetry axes with increasing jump frequency Ω: a) $\Omega = 5$ kHz, b) $\Omega = 10$ kHz, c) $\Omega = 15$ kHz, d) $\Omega = 45$ kHz, e) $\Omega = 140$ kHz.

Figure 5 shows the evolution of the spectrum with increasing Ω_x. A central peak grows on increasing Ω_x while the width remains to be $6\nu_Q = 135$ kHz. For extreme narrowing, i.e. when $\Omega_x \gg \Delta\nu_{rig}$ ($1C_2^\infty$ case) (34) has to be written in the equivalent form

(35)

$$\dot{\varrho}_1 = -i\bar{\nu}'\varrho_1 + \Omega_2(\varrho_3+\varrho_4-2\varrho_1) + \Omega_3(\varrho_2+\varrho_4-2\varrho_1) + \Omega_4(\varrho_2+\varrho_3-2\varrho_1) + \Omega_y(\varrho_4-\varrho_1) + \Omega_z(\varrho_2-\varrho_1),$$

$$\dot{\varrho}_2 = -i\bar{\nu}''\varrho_2 + \Omega_1(\varrho_3+\varrho_4-2\varrho_2) + \Omega_3(\varrho_1+\varrho_4-2\varrho_2) + \Omega_4(\varrho_1+\varrho_3-2\varrho_2) + \Omega_y(\varrho_3-\varrho_2) + \Omega_z(\varrho_1-\varrho_2),$$

$$\dot{\varrho}_3 = -i\bar{\nu}'\varrho_3 + \Omega_1(\varrho_2+\varrho_4-2\varrho_3) + \Omega_2(\varrho_1+\varrho_4-2\varrho_3) + \Omega_4(\varrho_1+\varrho_2-2\varrho_3) + \Omega_y(\varrho_2-\varrho_3) + \Omega_z(\varrho_4-\varrho_3),$$

$$\dot{\varrho}_4 = -i\bar{\nu}''\varrho_4 + \Omega_1(\varrho_2+\varrho_3-2\varrho_4) + \Omega_2(\varrho_1+\varrho_3-2\varrho_4) + \Omega_3(\varrho_1+\varrho_2-2\varrho_4) + \Omega_y(\varrho_1-\varrho_4) + \Omega_z(\varrho_3-\varrho_4),$$

where $\bar{\nu}' = \frac{1}{2}(\nu_1+\nu_3)$ and $\bar{\nu}'' = \frac{1}{2}(\nu_2+\nu_4)$.

The spectrum reveals the shape characteristic of the asymmetric EFG tensor ($\bar{\eta}=1$) and $\bar{\nu}_Q = 3\nu_Q$ [21], a dynamic average in this case.

If the next consecutive axis activated with increasing temperature was the second C_2 axis, the spectrum would narrow, as is easy to show, to a single central Lorentzian line. When, however, the next axis activated is a threefold one, the line shape passes an evolution, and for the extreme narrowing ($1C_2^\infty\, 1C_3^\infty$) assumes the shape presented in Figure 6. The activation of the consecutive threefold axes in a sequence makes the spectrum in the extreme narrowing limit three times narrower for each following C_3 axis (see explanation given in the legend of Figure 6).

Equivalent Axes

The case in which at least two of seven activation barriers characterizing the motion of the ion in crystal lattice are equal is rather uninteresting, although often encountered in real crystals of ammonium salts mainly with higher point symmetry (e.g. cubic). Then the evolution of the spectrum beginning with the rigid lattice shape evolves through a superlorentzian line without any structure into a single central Lorentzian line (Figure 7). Jumps about at least two different axes with the same jump frequency lead to equal probability for a deuteron of being in each of four sites in ND_4^+ tetrahedron. The average Hamiltonian in such a case is just zero.

IV. Discussion of Some Literature Results

Motional dynamics of ammonium ions was as subject of numerous studies by various methods. The ions, located in local crystalline fields of various symmetry, may exhibit features due to tunneling at low temperatures and the reorientation by thermally activated jumps at high temperatures [27]. For both ranges, taking deuteriated ammonium ions brings some attractive advantages when NMR spectroscopy is applied. We can therefore find some published spectra at high temperatures and wish to propose a new interpretation for them.

An external EFG, comming from a noncubic arrangement of charges around the ion, introduces a structure related contribution to the effective quadrupole interaction of deuterons, which may be visible on the deuteron spectra. Introduction of the external EFG for each deuteron was found necessary for the explanation of the tunneling ND_4^+ spectra measured for ND_4ClO_4 single crystal. At about 50 K a narrow doublet representing the "$4C_3^\infty - C_2^\infty$" case shows an angular dependence ($3\cos^2\Theta - 1$). As Θ is defined between

$\vec{B}_0$ and the direction of the primary C_3 axis, its direction in the crystalline field had been found. It confirms the approach of the present study, but particulars will be given elsewhere [28].

Narrow doublets were observed in $Rb_x(ND_4)_{1-x}D_2PO_4$ mixed single crystals [29]. The quadrupole coupling constant 3.7 kHz was measured over a large temperature range and various compositions, for which a powder doublet with $\delta = 2.7$ kHz would emerge. We proposed the sequence "$4C_3^\infty - C_2^\infty$" as a description of the ammonium ion mobility, which is compatible with the tetrahedral crystal structure. The doublet characteristic for the "$4C_3^\infty - C_2^\infty$" sequence was observed for some other powder samples of ammonium compounds.

The geometry of the trimethylamine molecule and, in consequence, the motional averaging in the spectra bear some similarity to the ammonium ion case. Methyl group C_3 axes make the tetrahedral angles among themselves and with a C_3' axis of the whole molecule. One C–D direction per methyl group appears to be coaxial with the C_3' axis. Fast C_3' reorientation leaves the spectra of these deuterons intact as a background for the narrowed to $\frac{1}{3}$ spectrum of the remaining deuterons. Additional fast reorientation of methyl groups gives a doublet spectrum of $\frac{1}{9}$ rigid width [19]. As we see, averaging by two independent reorientations gives a spectrum equivalent to our "$2C_3^\infty$" sequence. However, the existence of the fourth deuteron in ND_4^+, immobile during each C_3 reorientation and contributing to a second component, rules out the use of intermediate range results for our purpose.

ND_4NO_3 supplies a very interesting example of a compound having several structural phases, each with a characteristic ^{2}H-NMR spectrum. The deuteron spectra [25] and T_1 [30] were measured some time ago and repeated recently [31]. Based on our model, we propose the following interpretation of published spectra: In phase I ($T > 400.7$ K) the spectra are very narrow ($\delta \sim$ field inhomogeneity) indicating the ND_4^+ ion migration in a lattice. On transition to phase II ($400.7 > T > 366.2$ K) the translational diffusion is slowed down. Isotropic reorientation of ions is still present and leaves the spectrum narrow and structurless ($\delta \sim 0.7$ kHz). In phase III ($366.2 > T > 308.7$ K) the spectrum has the form shown in Figure 6 and exhibits no temperature dependence. Its width ($\delta \sim 2$ kHz) indicates the "$C_2^\infty - 4C_3^\infty - C_2^\infty$" model. In phase IV ($308.7 > T > 255.5$ K) the spectrum seems to be a sum of two superimposed components "$C_2^\infty - 3C_3^\infty - C_2^\infty$" and "$4C_3^\infty - C_2^\infty$" with about 4:1 ratio of intensities. On transition to phase V ($T < 255.5$ K) the spectrum clearly transforms into the "$C_2^\infty - 3C_3^\infty - C_2^\infty$" case. The width depends on temperature first just slightly, but below 150 K starts to increase rapidly. This indicates the jump rates for separate axes approaching the intermediate range, but their hierarchy cannot be guessed yet. The analysis of features in the spectra may be supported by a relaxation study, and some preliminary observations can be made on existing data [30]. There is only one step observed in the spin-lattice relaxation rates of both protons and deuterons on the transition between phases IV and III, indicating a structural change. The activation energy also changes at this point and amounts to about 12.8 kJ/mol in phases IV and V (down to about 160 K) for NH_4^+ as well as for ND_4^+. One can not exclude the existence of some new phases at still lower temperatures. Below about 160 K the activation energy changes again, and $E_a = 10.7$ kJ/mol and 8.6 kJ/mol were obtained for ND_4^+ and NH_4^+, respectively [30]. The change in the activation energy is apparent. Its decrease with decreasing temperature indicates a continuous transition from relaxation dominated by C_2 reorientations to a contribution of C_3 reorientations against a lower barrier.

The pioneering work of Chiba [21] reports on ^{2}H-NMR spectra of ND_4IO_3 and $(ND_4)_2SO_4$ just below room temperature. The case of ND_4IO_3 we interpret as "$C_2^\infty - 3C_3^\infty - C_2^\infty$", since it clearly resembles the spectrum of Fig. 6 with a width of about 5 kHz. The $(ND_4)_2SO_4$ spectrum is most probably a sum of "$C_2^\infty - 3C_3^\infty - C_2^\infty$" and "$C_2^\infty - 4C_3^\infty - C_2^\infty$" types. Ammonium ions are in this case occupying two sites different in symmetry and barrier height [14].

The interpretation of experimental data presented here is certainly preliminary. A careful verification of our interpretation will be given on the basis of new measurements. Besides, a model has to be developed that would include a statistical interpretation of composed spectra. Work along these lines is being continued.

V. Conclusions

Following previous mumerous studies we report findings concerning the unique possibilities of deuteron NMR spectroscopy for resolving and clarifying the nature of molecular motions and for determining separate reorientation rates. We owe these

possibilities to the value and transformation properties of the deuteron quadrupole Hamiltonian under symmetry rotations of a molecule. Features in the ^{2}H-NMR spectra of reorienting ND_4^+ ions are considered. We for the first time point out the sequential character of multiaxial reorientation of molecules with no internal degrees of freedom. Their symmetry rotations cannot be simultaneously executed, which results in motional dynamics seen in detail as a series of statistically uncorrelated jumps about some axes with different correlations frequencies.

Calculated spectra serve as a guidance in pointing out important features of a motional model. Computations for primary C_3 or C_2 axis reorientation refer to cases of asymmetric threedimensional potentials, when one axis reorientation prevails. We obtained different spectra in these two cases. For one axis reorientation in the extreme narrowing limit the spectra presented here are identical with those calculated before for very high tunneling frequencies about respective single axes. However, clearly distinguishable spectra are observed in the intermediate ranges of the correlation and tunneling frequencies [32].

When one axis reorientation becomes interrupted by jumps about any other axis, which under experimental conditions happens due to increasing temperature, the spectra bear still a mark of the primary motion. A number of possible sequences like "$n\,C_3^\infty - x\,C_2^\infty$" or "$C_2^\infty - n\,C_3^\infty - x\,C_2^\infty$" ($n = 1, 2, 3, 4, \quad x = 0, 1$) lead to spectra different in shape and/or width.

Sequential multiaxis reorientation may be observed experimentally for ND_4^+ in low symmetry potentials securing a hierarchy of axes in terms of respective activation energies. The plateau found in the temperature dependence of the spectral width (or of the second moment) can be labelled with unambiguously attributable sequences of single axis reorientations. Higher symmetry cases show transitions from a rigid ion spectrum to a very narrow line for a sequence sometimes lacking just one symmetry rotation. A direct transition from the rigid doublet to the isotropically narrowed spectrum is a common observation for cubic potentials.

The concepts outlined above are verified on some previously published experimental examples. A set of cases was chosen to represent some of possible categories. Sequences lead by primary C_3 or C_2 reorientations have their respective representation. As expected, such spectra do not change over, sometimes, wide range of temperatures. A systematic decrease in width is observed and may be attributed to an increasing amplitude of torsional oscillations about equilibrium orientations. The spectra obtained for different crystalline phases of a compound indicate possible structural conclusions. However, in spite of a clear change at phase transition, due to still limited data one cannot yet unequivocaly judge the extent of possible structural information.

Various cases of ND_4^+ ions mobility, clearly observed on the spectra, may exhibit related features in the spin-lattice relaxation. Contributions of reorientations about separate axes against different barriers change with temperature, and those fulfilling the condition $\nu_0 \Omega^{-1} \sim 1$ dominate. Related features in the spin-lattice relaxation, as changing slopes and broadened minima, may result. When not related to a structural phase transition, changes of activation energy on temperature may therefore be apparent. Particularly clear are the cases where separate minima can be observed in spite of equivalence of positions for all ions, thus indicating a large difference in the barrier height for some reorientation axes. Such correlations between the features of spectra and relaxation confirms our approach.

On the basis of the analysis of spectra, we indicate here some possibilities of distinguishing between different multiaxis sequential motions of ND_4^+. The first presentation of the subject, extensive as it is, does not cover all observable cases, and the work will be continued.

Acknowledgement

Preliminary measurements, important for the development of the ideas presented, were performed in collaboration with L. P. Ingman, E. Koivula, E. E. Ylinen, and A. Birczyński. The authors highly appreciate fruitful discussions with J. W. Hennel, M. Punkkinen, and T. Abesadze.

[1] G. E. Pake, J. Chem. Phys. **16,** 327 (1948).
[2] E. R. Andrew, R. Bersohn, J. Chem. Phys. **18,** 159 (1950).
[3] H. S. Gutowsky, G. E. Pake, R. Bersohn, J. Chem. Phys. **22,** 643 (1954).
[4] H. W. Spiess, Adv. in polymer sci. **66,** 23 (1965).
[5] K. Beshah, E. T. Olejniczak, R. G. Griffin, J. Chem. Phys. **86,** 4730 (1987).
[6] Z. Luz in NMR of Liquid Crystals, J. W. Emsley Ed. (Reidel, NY 1985), p. 315.
[7] M. Lausch, H. W. Spiess, J. Mag. Res. **54,** 466 (1983).
[8] A. K. Roy, A. A. Jones, P. T. Inglefield, J. Mag. Res. **64,** 441 (1985).
[9] M. S. Greenfield, A. D. Ronemus, R. L. Vold, R. R. Vold, P. D. Ellis, T. E. Raidy, J. Mag. Res. **72,** 89 (1987).
[10] B. Berglund, J. Tegenfeldt, J. Mag. Res. **27,** 315 (1977).
[11] C. Müller-Rowat, U. Haeberlen, J. Rowat, J. P. Colpa, Chem. Phys. **96,** 327 (1985).
[12] A. Keller, S. Benz, U. Haeberlen, J. Mag. Res. **72,** 434 (1987).
[13] R. G. Griffin, Meth. Enzymol. **72,** 108 (1981).
[14] D. J. Genin, D. E. O'Reilly, J. Chem. Phys. **50,** 2842 (1969).
[15] J. A. Ripmeester, C. I. Ratcliffe, J. Chem. Phys. **88,** 1053 (1985).
[16] S. Mooibroek, R. E. Wasylishen, Can. J. Chem. **63,** 2926 (1985).
[17] S. Nishikiori, R. I. Ratcliffe, J. A. Ripmeester, J. Phys. Chem. **94,** 8098 (1990).
[18] C. M. Gall, J. A. DiVerdi, S. J. Opella, J. Am. Chem. Soc. **103,** 5039 (1981).
[19] A. J. Vega, Z. Luz, J. Chem. Phys. **86,** 1803 (1987).
[20] I. C. P. Smith, in NMR: Principles and Applications to Biomedical Research, J. W. Pettegrew, Ed., Springer Verlag, 1989, p. 124.
[21] T. Chiba, J. Chem. Phys. **36,** 1122 (1962).
[22] T. Chiba, Bull. Chem. Soc. Japn. **38,** 490 (1965).
[23] S. Chen, D. C. Ailion, Phys. Rev. **B42,** 5945 (1990).
[24] L. P. Ingmann, E. Koivula, Z. T. Lalowicz, M. Punkkinen, E. E. Ylinen, Z. Phys. B-Condensed Matter **66,** 363 (1987).
[25] V. Hovi, U. Järvinen, P. Pyykkö, Ann. Acad. Sci. Fenn. **AVI,** No. 221 (1966).
[26] J. Kaplan, G. Fraenkel, NMR of Chemically Exchanging Systems, Academic Press, NY, 1980.
[27] L. P. Ingmann, E. Koivula, Z. T. Lalowicz, M. Punkkinen, E. E. Ylinen, J. Chem. Phys. **88,** 58 (1988).
[28] A. Birczyński, Z. T. Lalowicz, M. Punkkinen, E. E. Ylinen (to be published).
[29] R. Blinc, J. Dolinšek, V. H. Smidt, P. C. Ailion, Europhys. Lett. **6,** 55 (1988).
[30] L. Niemelä, T. Lohikainen, Phys. kondens. Materie **6,** 376 (1967).
[31] R. Grosescu, U. Haeberlen, M. Lupu, Rev. Roum. Phys. **3,** 637 (1988).
[32] Z. T. Lalowicz, Z. Naturf. **43a,** 895 (1988).